© 2021 The Authors
793

Water Practice & Technology Vol 16 No 3
doi: 10.2166/wpt.2021.034

Coffee residue-based activated carbons for phenol removal

Hemavathy Palanisami[a], Mohamad Rafiuddin Mohd Azmi[a], Muhammad Abbas Ahmad Zaini[a,b,*], Zainul Akmar Zakaria[a], Muhd Nazrul Hisham Zainal Alam[a] and Mohd Azizi Che Yunus[a,b]

[a] School of Chemical & Energy Engineering, Faculty of Engineering, Universiti Teknologi Malaysia, 81310 UTM, Johor Bahru, Johor, Malaysia

[b] Centre of Lipids Engineering & Applied Research (CLEAR), Ibnu-Sina Institute for Scientific & Industrial Research, Universiti Teknologi Malaysia, 81310 UTM, Johor Bahru, Johor, Malaysia

*Corresponding author. E-mail: abbas@cheme.utm.my

Abstract

This work was aimed to evaluate the adsorptive properties of activated carbons from coffee residue for phenol removal. The coffee residue was activated using H_3PO_4 and KOH, and the resultant activated carbons were characterized for surface area and functional groups. The values of surface area were recorded as 1,030 m^2/g and 399 m^2/g for H_3PO_4- and KOH-activated carbons, respectively. The maximum capacity for phenol removal is comparable for both activated carbons at 43 mg/g. The pores might be inaccessible due to electrostatic repulsion by surface functional groups and hydroxyl anions. The second stage in a two-stage adsorber design is necessary to accomplish the process with high performance and minimum dosage of activated carbon. Coffee residue is a promising activated carbon precursor for phenol removal.

Key words: activated carbon, adsorption, coffee residue, phenol, two-stage adsorber

Highlights

- Coffee residue was activated using phosphoric acid or potassium hydroxide.
- Activated coffee residue carbons exhibit phenol capacity of 43 mg/g.
- Two-stage adsorber offers insight into high performance and minimum adsorbent dosage.

INTRODUCTION

The demand for phenol-related products has resulted in the manufacturing of phenol in large scale. One of the major products is phenolic resin, which is produced through polymerization reaction of formaldehyde with phenol. The use of large amounts of phenol in processing may eventually result in the chemical finding its ways to the environment. Phenol is highly poisonous to living beings (Anku *et al.* 2017). Therefore, the effluent bearing the chemical must be fully treated before it enters the water bodies. Various treatment methods such as coagulation/flocculation, precipitation, membrane filtration, reverse osmosis, ozonation, advanced oxidation processes and ion exchange have been used for the elimination of organic pollutants in wastewater (Shu-Hui & Zaini 2016; Anku *et al.* 2017; Crini & Lichtfouse 2019). However, these techniques have several limitations, as they involved the use of chemicals and often resulted in secondary pollution.

Water Practice & Technology Vol 16 No 3
doi: 10.2166/wpt.2021.034

Among others, adsorption has emerged as a preferred treatment for wastewater because the process is simple and straightforward, inexpensive, consumes low energy, and produces minimum sludge. Activated carbon is a widely used adsorbent in adsorption. It is a material that is produced from carbonaceous precursors, such as coal, coconut shell, wood, and lignite (Ming-Twang *et al.* 2015).

Coffee is produced everywhere worldwide. Consequently, the leftover of coffee drink; that is, the coffee residue, is abundantly available. Because it has no commercial value, coffee residue could be a sustainable resource of activated carbon for wastewater treatment (Laksaci *et al.* 2017). Moreover, without proper solid waste management and disposal, the waste material may well lead to other environmental issues.

To date, there is still limited literature available to unlock the true potential of coffee residue as activated carbon, and its two-stage adsorber design in evaluating the efficiency of phenol removal. Castro and co-workers (Castro *et al.* 2011) reported the removal of phenol at 150 mg/g by coffee grounds activated using potassium carbonate and steam. In a related work, Khenniche & Benissad-Aissani (2010) showed an 85 mg/g phenol removal by zinc chloride-activated coffee residue. Hence, the present work was aimed to establish the adsorptive properties of coffee residue-based activated carbons by phosphoric acid or potassium hydroxide activation so as to enrich the body of present knowledge. The two-stage design would bring useful insight into dosage optimization and practical applications of batch adsorption. The findings and mechanisms of phenol adsorption are discussed.

MATERIALS AND METHODS

Materials

Coffee residue was obtained from a Starbucks outlet in the Johor state of Malaysia. Potassium hydroxide and phosphoric acid (85%) were supplied by QRec (Asia) and R&M Chemicals, respectively. Phenol (99%) was purchased from Sigma-Aldrich. All chemicals were of analytical grade and were used as received without further purification.

Chemical activation

Coffee residue was oven-dried at 100 °C for 24 h. It was mixed with H_3PO_4 or KOH at mass ratio of 1:1. Distilled water was added into the mixture to ensure it was homogeneously stirred for 30 min. The mixture was completely dried in an oven for impregnation prior to activation in a furnace under anoxic environment at 600 °C for 1.5 h. The activated carbons were refluxed with distilled water for 24 h to remove unreacted reagents. The resultant activated carbons were designed as SA and SB for H_3PO_4- and KOH-activated carbons, respectively.

Characterization of materials

The thermal decomposition profile of materials studied was obtained using a Perkin-Elmer thermogravimetric analyzer (TGA 7) under nitrogen flow of 10 mL/min and heating rate of 15 °C/min. The specific surface area of activated carbons was determined using a Micromeritics surface area analyzer (ASAP 2020) at a liquid nitrogen temperature of 77 K. The surface chemistry of coffee residue and its derived activated carbons was qualitatively determined using a Perkin Elmer FTIR spectrometer (Spectrum One). The surface morphology of activated carbons was characterized using a Hitachi scanning electron microscope (TM3000). The pH coffee residue based activated carbons were measured using a portable pH meter (HI 9813-5, Hanna Instruments). Briefly, 10 g of sample was

Water Practice & Technology Vol 16 No 3
doi: 10.2166/wpt.2021.034

immersed in 100 mL of distilled water, the mixture was heated for 15 min and allowed to cool at room temperature prior to pH measurement.

Adsorption studies

The adsorptive properties of activated carbons were evaluated at different phenol concentrations and contact times using a bottle-point technique. Three replicates were performed, and the average values were reported. A 50 mg of activated carbon was added into 50 mL of phenol solution of varying concentrations ranging between 5 mg/L to 500 mg/L. The mixture was allowed to equilibrate for 72 h. The residual concentrations were measured using a Drawell UV-Vis spectrophotometer (DU-8200) at a wavelength of 270 nm. The calibration standard was determined as a.u. $= 0.0229\times$ concentration, for 0 mg/L $<$ phenol concentration $<$25 mg/L with $R^2 = 0.9985$. The adsorption capacity was calculated from mass balance,

$$q_e = \frac{V}{m}(C_o - C_e) \tag{1}$$

where, q_e (mg/g) is the equilibrium adsorption, V (L) is the volume of phenol solution, m (g) is the mass of activated carbon, C_o (mg/L) is the initial concentration and C_e (mg/L) is the equilibrium concentration. The equilibrium data were analyzed using Langmuir and Freundlich models, as follows

$$q_e = \frac{q_m b C_e}{1 + bC_e} \tag{2}$$

$$q_e = K_F C_e^{\frac{1}{n}} \tag{3}$$

where, q_m (m/g) is the maximum adsorption capacity, b (L/mg) is the adsorption affinity, and K_F and n are Freundlich constants.

The rate of adsorption was performed at concentrations of 5 mg/L and 20 mg/L. A 50 mg of activated carbon was brought into intimate contact with 50 mL of phenol solution, and the concentration of phenol was measured at different time intervals until the constant reading was attained. The adsorption capacity at time, t, q_t (mg/g) was calculated as

$$q_t = \frac{V}{m}(C_o - C_t) \tag{4}$$

where, C_t (mg/L) is the concentration at time, t. The kinetics data were analyzed using pseudo-first-order and pseudo-second-order models as follows

$$q_t = q_e(1 - e^{-k_1 t}) \tag{5}$$

$$q_t = \frac{q_e^2 k_2 t}{1 + q_e k_2 t} \tag{6}$$

where, k_1 and k_2 are rate constants for pseudo-first-order and pseudo-second-order models, respectively. The isotherm and kinetic models were solved through non-linear regression using *Solver* of MS Excel. The sum of squared error (SSE) was set minimum to yield optimum coefficient of determination, R^2.

Water Practice & Technology Vol 16 No 3
doi: 10.2166/wpt.2021.034

Two-stage adsorber design

The two-stage adsorber design is aimed to optimize the activated carbon used in adsorption. The schematic representation of the two-stage batch adsorption process is shown in Figure 1.

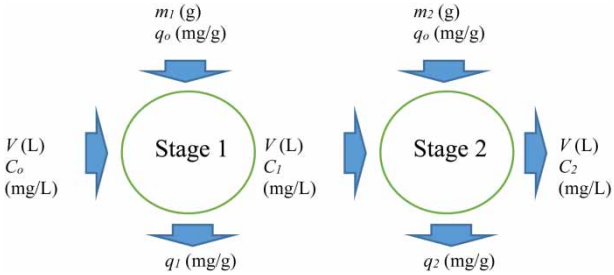

Figure 1 | Two-stage adsorber design.

The following expression for mass of activated carbon required for adsorption was obtained by combining the adsorption capacity in Equation (1) with Langmuir model in Equation (2).

$$m = \frac{V}{q_m b C_e}(C_o - C_e)(1 + bC_e) \tag{7}$$

For two-stage process, the total activated carbon mass is

$$m_1 + m_2 = \frac{V}{q_m b C_1}(C_o - C_1)(1 + bC_1) + \frac{V}{q_m b C_2}(C_1 - C_2)(1 + bC_2) \tag{8}$$

where, C_1 is the concentration leaving stage 1 and becomes the feed for stage 2, and $C_2 = C_e$. The optimum mass can be calculated by differentiating Equation (8) with respect to C_1.

$$\frac{d(m_1 + m_2)}{dC_1} = 0 \tag{9}$$

Solving

$$C_1 = (C_o C_2)^{0.5} \tag{10}$$

The performance of two-stage adsorber can be calculated as

$$Removal\ (\%) = \frac{C_o - C_2}{C_o} \times 100 \tag{11}$$

Different constraints were set to allow comparison of the amount of activated needed in a single stage adsorber to that of a two-stage adsorber.

RESULTS AND DISCUSSION

Characteristics of materials

Figure 2 shows the thermogravimetric profiles of coffee residue (CR) and activated carbons. Coffee residue exhibits a high weight loss of 81% at 860 °C, with sharp peak centred at 310 °C. In anoxic

Water Practice & Technology Vol 16 No 3
doi: 10.2166/wpt.2021.034

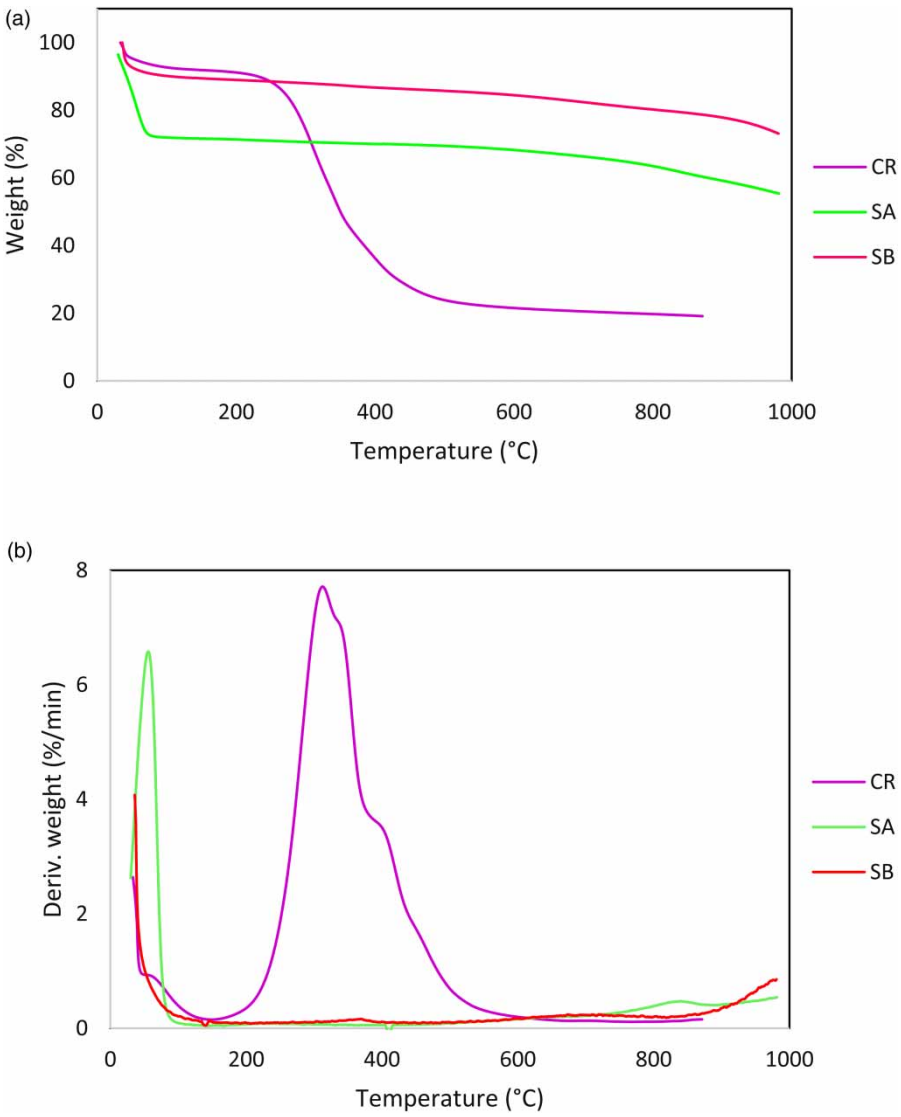

Figure 2 | Thermogravimetric profiles of coffee residue and activated carbons, (a) weight loss, (b) derivative weight loss.

environment, the weight of coffee residue is stabilized at 600 °C, which is also the activation temperature. The pyrolysis of carbonaceous material normally gives rise to char, oil (tar) and gas phases. A rudimentary porosity is obtained because of the release of volatiles such as hydrogen, oxygen, and nitrogen, leaving a rigid carbon skeleton formed by aromatic structures. Activated carbons display a thermal resistant behaviour with weight loss of 27 and 44% for SB and SA, respectively. A greater weight loss of the latter could be explained by the presence of well-developed porous structure that easily entrapped moisture from the surrounding and collapsed at high temperature. The weight loss at about 100 °C is generally attributed to the elimination of physisorbed moisture, while that at 400 °C corresponds to the release of volatiles and decomposition of the oxygenated surface groups (Laksaci *et al.* 2017).

Figure 3 shows the nitrogen adsorption-desorption isotherm profiles of activated carbons, and the textural properties are summarized in Table 1. SA displays a Type I isotherm according to IUPAC classification, indicative of the presence of micropores. The shape of hysteresis loop is often assigned to specific pore structure. Most of nitrogen adsorption for SA occurs at $P/P_o < 0.4$, with hysteresis loop of H4 for the reduced pressures above 0.4. This can be attributed to capillary condensation in narrow slit-shaped mesopores, implying that this activated carbon possesses both micropores and

Water Practice & Technology Vol 16 No 3
doi: 10.2166/wpt.2021.034

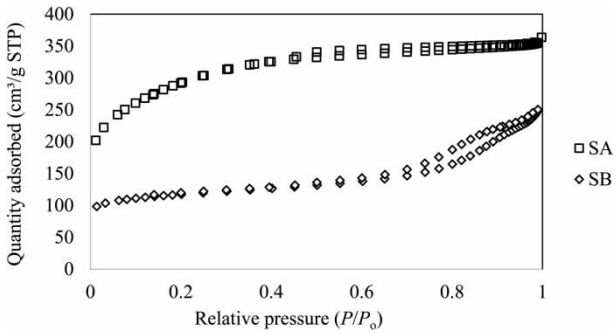

Figure 3 | N_2 adsorption/desorption isotherm profiles of coffee residue activated carbons.

Table 1 | Textural properties of activated carbons

Samples	SA	SB
Yield (%)	41.2	17.5
pH	4.00	9.00
BET surface area (m^2/g)	1,030	399
Micropore area (m^2/g)	364	264
Mesopore area (m^2/g)	665	136
Micropore volume (cm^3/g)	0.160	0.122
Mesopore volume (cm^3/g)	0.387	0.253
Total pore volume of pores (cm^3/g)	0.547	0.375
Average pore diameter (nm)	2.13	3.76
Micropore content (%)	29.3	32.5

mesopores. SB shows a predominantly Type IV isotherm, the characteristic of mesoporous material. SB also exhibits a hysteresis loop of H4 within the P/P_o range from 0.65 to 1 (Sing 1982). A horizontal adsorption plateau is observed at higher P/P_o, suggesting that the micropores are dominant in activated carbon. The desorption isotherm which shows a deviation from the adsorption isotherm can be explained by the presence of bottleneck or slit pores (Rouquerol *et al.* 2013).

From Table 1, SA shows a high specific surface of 1,030 m^2/g, which is more than 2.5 times that of SB. SA possesses a narrow pore size distribution, located mainly in the microporous domain with D_p of 2.13 nm. Apart from surface area and porosity, the accessibility of reactive centres on the carbon surface is also important for adsorption. The surface is acidic (pH 4.0) for SA and alkaline (pH 9.0) for SB. The acidic character of SA could be attributed to H_3PO_4 activation that caused the deposition of oxygen functional groups, while the surface accumulation of hydroxyl anions renders the basic character to SB (Arampatzidou & Deliyanni 2016). The yield of SB is comparatively small at 17.5% than that of SA, because KOH is a strong dehydrating agent that enhances the carbon burning-off (Hui & Zaini 2015). As coffee residue is readily in powder form, it is easily decomposed, giving low yield and low surface area.

The elemental composition of coffee residue activated carbons is summarized in Table 2. Coffee residue originally contained 52.0% carbon, 7.54% hydrogen, 2.29% of nitrogen and 38.0% of oxygen (by difference). Upon activation, the carbon content increased to 57.3–57.7%, while the hydrogen content decreased to 2.21–3.97%. In KOH activation, the oxygen content increased due to the decomposition of metal hydroxide into oxides within the carbon matrix and the formation of oxygen functional groups on the surface of activated carbon (Hui & Zaini 2015). The sulfur content decreased in SA (0.176%) but increased in SB (0.312%) because of the volatility of this element. The

Water Practice & Technology Vol 16 No 3
doi: 10.2166/wpt.2021.034

Table 2 | Elemental composition of coffee residue and activated carbons

Sample	Element (%)					C/H ratio	C/N ratio
	C	H	N	S	O		
CR	52.0	7.54	2.29	0.193	38.0	6.89	22.7
SA	57.7	3.97	2.56	0.176	35.6	14.5	22.5
SB	57.3	2.21	1.91	0.312	38.3	25.9	30.1

C/H ratio of coffee residue increased upon activation, signifying the formation of rich carbon (graphitic) structure, while the C/N ratio implies that the amount of nitrogen mostly retained after the activation.

The SEM images of activated carbons showing the heterogeneous surface and porous nature are shown in Figure 4. The cracks, voids, and crevices as observed from the morphology act as the entrance of pore channels for microporous-mesoporous network of activated carbon (Laksaci *et al.* 2017). The external surface of SA displays some crater-like and non-uniform honeycomb-like pore entrances. They are visible because the specific surface is high (1,030 m^2/g). SB exhibits a smooth sponge-like texture as a result of the effect of the dehydrating agent during heat treatment.

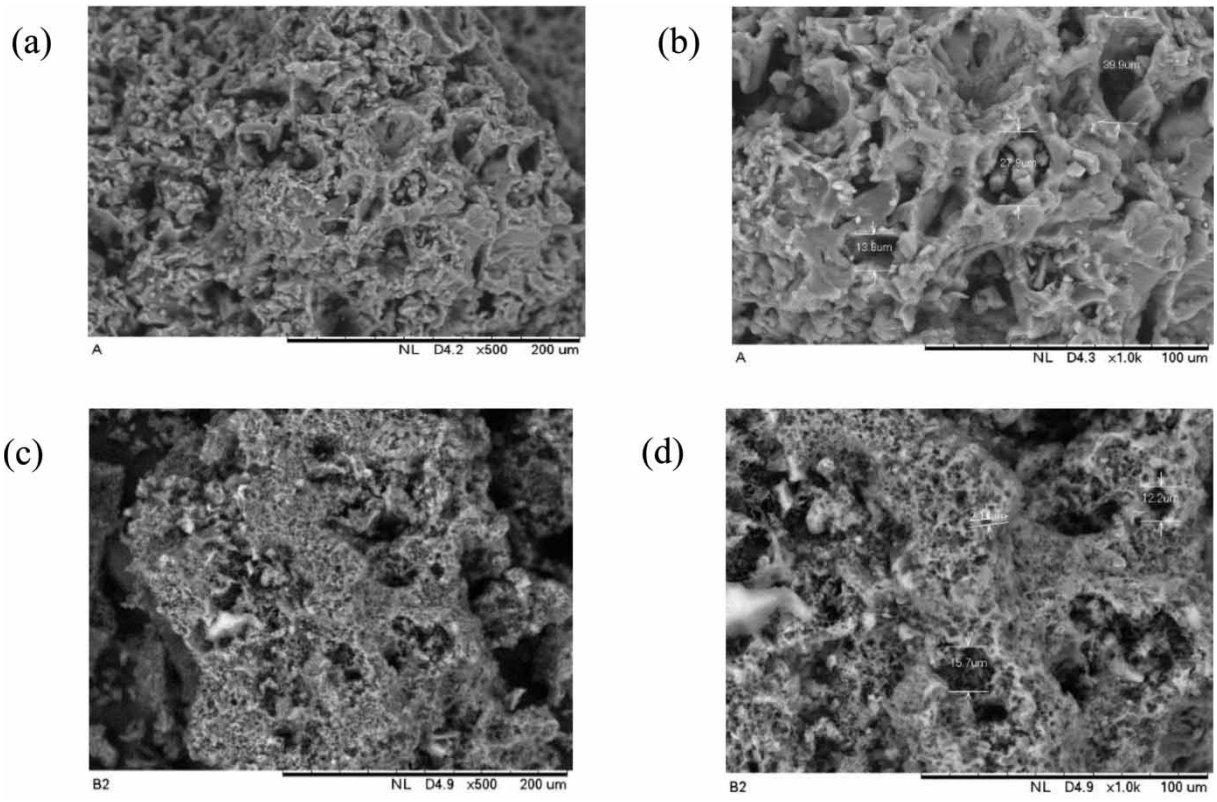

Figure 4 | SEM images of ((a) and (b)) SA and ((c) and (d)) SB at ×500 ((a) and (c)) and ×1,000 ((b) and (d)) magnifications.

Figure 5 shows the FTIR spectra of coffee residue and activated carbons. The spectrum of coffee residue displays multiple peaks of varying intensity, signifying a surface rich in functional groups, while the spectra of activated carbons are simplified, with missing peaks and some of decreasing intensity owing to the decreasing amount of functional groups remaining on the carbon surface upon chemical activation. The broad absorption band at 3,600–3,300 cm^{-1} indicates the stretching

Water Practice & Technology Vol 16 No 3
doi: 10.2166/wpt.2021.034

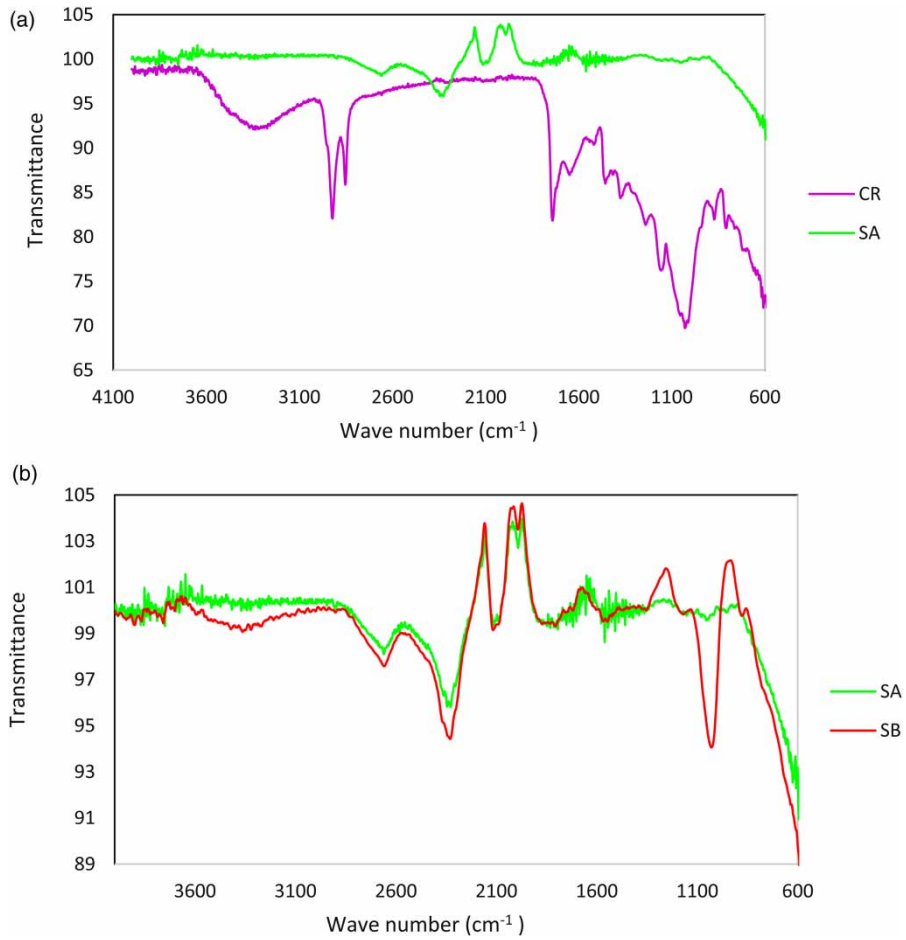

Figure 5 | FTIR spectra of coffee residue and activated carbons.

vibration of hydrogen-bonded hydroxyl groups (from carboxyl, phenols or alcohols) and moisture (Laksaci *et al.* 2017). Two peaks of C–H stretching were observed at 2,922 cm^{-1} and 2,853 cm^{-1}, correspond to asymmetric and symmetric stretching of alkane compound. The band at 1,740 cm^{-1} can be attributed to the C = O stretching vibration of acetyl and uronic ester groups (a class of sugar acids containing carbonyl and carboxylic acid) of hemicellulose (Wang *et al.* 2009). The peak at 1,635 cm^{-1} signifies the carboxyl linkage derived from xanthine derivatives such as caffeine (Lyman *et al.* 2003). The FTIR spectra of SA and SB show absorption bands representing the aliphatic C–H stretching in aromatic methoxyl group, and methyl and methylene groups of side chains. The absorption band at 1,028 cm^{-1} signifies the C–OH bending and CH_2 related modes. The band at around 2,350 cm^{-1} can be attributed to the stretching of C ≡ C.

Adsorption studies

Figure 6 shows the adsorption kinetics of phenol by coffee residue activated carbons, and the kinetic constants are summarized in Table 3. Generally, the removal of phenol displays an increasing trend with increasing contact time to a point of equilibrium, at which the rate of adsorption is equal to the rate of desorption. The adsorption rate is slower at higher concentration, thus a longer contact time would be required to attain the equilibrium. However, the adsorption intensity (slope) increases with concentration because the concentration gradient offers the driving force to overcome the mass transfer resistance for a greater adsorption for the same contact time. The rate of adsorption tends to slow down and subsides to zero as the contact time increases due to insufficient driving force, and

Water Practice & Technology Vol 16 No 3
doi: 10.2166/wpt.2021.034

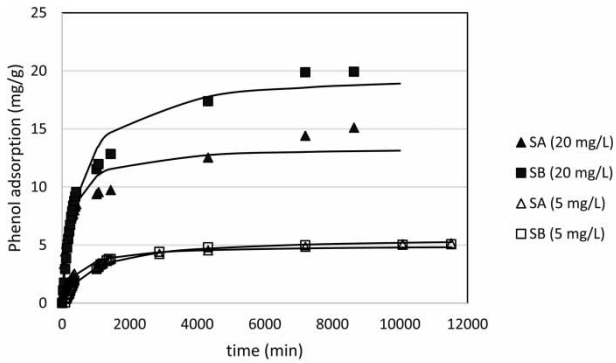

Figure 6 | Kinetics of phenol removal by coffee residue activated carbons.

Table 3 | Constants of pseudo-kinetics models

		Pseudo-first-order model				Pseudo-second-order model			
Sample	$q_{e,exp}$	q_e (mg/g)	$k_1 \times 10^{-3}$ (min^{-1})	R^2	SSE	q_e (mg/g)	$k_2 \times 10^{-4}$ (g/mg.min)	R^2	SSE
SA (5 mg/L)	5.24	4.42	2.03	0.913	5.69	4.98	5.03	0.975	1.54
SB (5 mg/L)	5.19	4.99	0.097	0.983	1.72	5.64	2.04	0.983	2.21
SA (20 mg/L)	15.1	11.9	3.54	0.875	37.0	13.4	3.16	0.943	16.3
SB (20 mg/L)	19.9	17.5	1.72	0.935	44.8	19.9	0.993	0.978	14.3

repulsion between the adsorbed phenol molecules and that in the bulk solution at equilibrium (Shaid *et al.* 2019).

From Table 3, both pseudo-kinetic models show a reasonably good fit to the experimental data with small variation between the experimental ($q_{e,\mathrm{exp}}$) and calculated values. At $C_o = 5$ mg/L, adsorption occurs mainly by physical diffusion, by which the mass transfer resistance is dominant. While, at $C_o = 20$ mg/L, the adsorption rate seems to obey the pseudo-second-order model, indicating a process controlled by physiochemical interactions (Shaid *et al.* 2019). For the concentrations studied, the adsorption increased in the order SA < SB, implying a faster saturation of SB, mainly due to its lower specific surface.

Figure 7 shows the equilibrium adsorption of phenol onto activated carbons, where the isotherm constants are summarized in Table 4. The adsorption capacity gradually increased with increasing concentration to a point of surface saturation. Both activated carbons display a comparable maximum capacity at about 43 mg/g (57% removal), despite the dissimilarity in surface area. This could be explained by the presence of acidic oxygen groups in SA and the basic surface of SB. The acidic

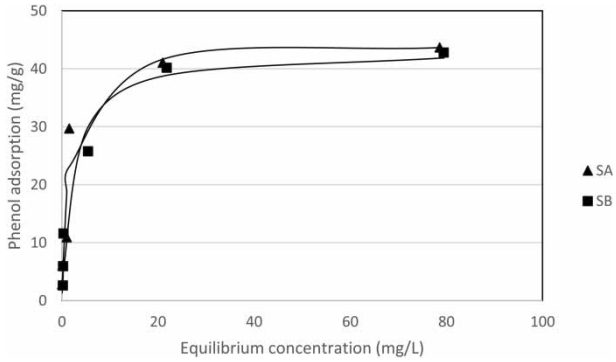

Figure 7 | Equlibrium adsorption of phenol by activated carbons.

Water Practice & Technology Vol 16 No 3
doi: 10.2166/wpt.2021.034

Table 4 | Constants of isotherm models

	SA	SB
$q_{m,\exp}$ (mg/g)	43.6	42.8
Langmuir model		
q_m (mg/g)	44.5	43.1
b (L/mg)	0.708	0.417
SSE	108	61.1
R^2	0.935	0.966
Freundlich model		
K_F	17.1	14.0
n	4.20	3.59
SSE	258	140
R^2	0.847	0.912

oxygen groups dissociate in water to produce the negatively charged surface of SA, while the surface of SB is surrounded by hydroxyl anions. Phenol in water can lose a hydrogen ion to form a more stable phenoxide ion, which carries the negative charge on the oxygen atom and delocalizes around the aromatic ring. This brings about an electrostatic repulsion that interferes with the accumulation of phenol molecules on the active sites. As shown in Figure 6, SA demonstrates a greater degree of repulsion than SB for a lower phenol removal at 20 mg/L, even though the former is high in surface area.

From Table 4, the Langmuir model fits the equilibrium data well with $R^2 > 0.94$, and proximity between the constant, q_m and the experimental data, implying the monolayer coverage of phenol molecules onto the homogeneous surface of activated carbon. Nonetheless, a slight deviation of model lines from the experimental data at higher concentration, as visualized in Figure 7, indicates that the removal of phenol could be governed by multilayer stacking of molecules, surpassing the restriction of electrostatic repulsion due to the high concentration gradient. In this work, the maximum phenol capacity of 43 mg/g by coffee residue-based activated carbons is comparable and sufficiently higher than that of organo-montmorillonite (50.1 m^2/g, 3.6 mg/g) (Wang *et al.* 2017), activated semicoke (347 m^2/g, 42.8 mg/g) (Gao *et al.* 2017), pine fruit shell char (228 m^2/g, 31.5 mg/g) (Mohammed *et al.* 2018), zeolite composite (872 m^2/g, 40.3 mg/g) (Cheng *et al.* 2016) and waste tyre activated carbon (237 m^2/g, 48 mg/g) (Shaid *et al.* 2019). Undeniably, some activated carbons from egg shell (113 m^2/g, 192 mg/g) (Giraldo & Moreno-Piraján 2014) and rubber seed shell (852 m^2/g, 302 mg/g) (Yan *et al.* 2019) recorded a superior removal of phenol due to favourable texture and surface charge for adsorption.

Two-stage adsorber design

A two-stage adsorber design was proposed for SB using the Langmuir model to minimize the amount of activated carbon required for phenol adsorption. For any volume of phenol to be treated, the two-stage batch adsorber is able to reduce nearly 14% of adsorbent dosage as compared to the single-stage adsorber. The required amounts of SB to reduce the effluent concentrations to 0.5–10 mg/g, and to achieve the performance of 80–99%, are visualized in Figure 8.

In Figure 8(a), C_1 is lower for a greater performance because of low equilibrium to compensate the remaining removal in the second stage. In other words, the amount of SB used in the first stage is higher for a higher target performance. As the phenol removal increased, the amount of SB also increased with C_o. From Figure 8(b), to achieve a 99.9% phenol removal, the minimum amounts of SB required for a two-stage adsorber are 90.6 and 547 g for $C_o = 50$ m/L and 350 mg/L, respectively.

Water Practice & Technology Vol 16 No 3
doi: 10.2166/wpt.2021.034

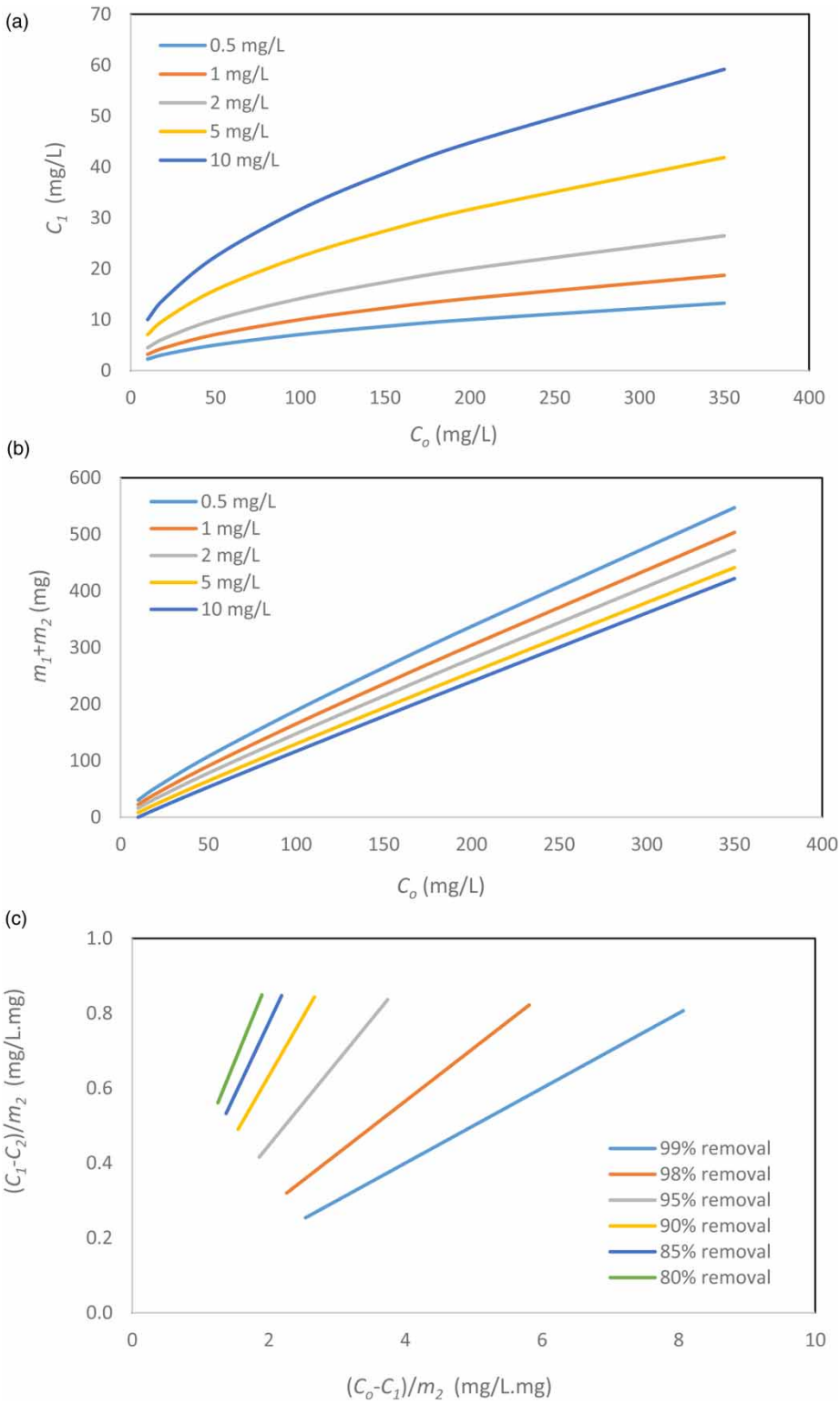

Figure 8 | (a) Intermediate concentration, C_1 against influent concentration, C_o; (b) combined mass of SB for various target effluent concentrations; (c) phenol removal in each stage for various removal performance.

In Figure 8(c), the efficiency for the second stage is always lower than that of the first stage, as C_1 is lower. Likewise, the efficiency for the first stage is significant for high removal performance using high C_o (Hijab *et al.* 2020). At high C_2, the efficiency of the second stage is minimal. However, the gap of efficiency in the second stage is broadened when the target performance is high, and the influent

Water Practice & Technology Vol 16 No 3
doi: 10.2166/wpt.2021.034

concentration is low. Therefore, adding a second stage even for low C_2 is essential to achieve the desired removal efficiency with minimum dosage of activated carbon.

CONCLUSION

Activated carbons were prepared from coffee residue using H_3PO_4 or KOH activation. The H_3PO_4-activated carbon exhibits a higher specific surface of 1,030 m^2/g. Nonetheless, both activated carbons demonstrate a similar phenol removal at 43 mg/g (57% removal) due to possible electrostatic repulsion. From the kinetics point of view, the KOH-activated carbon displays a less restricted barrier for a better phenol adsorption at $C_o = 20$ mg/L. The phenol adsorption could be governed by physicochemical interactions. In two-stage adsorber design, the efficiency of the first stage should be high enough to permit high performance for high phenol concentration, while the second stage is necessary to accomplish the process with minimum dosage of activated carbon. Coffee residue-based activated carbon could be useful for the removal of phenol in wastewater treatment.

ACKNOWLEDGEMENT

This work is financially supported by UTMShine Signature Grant No. 07G80.

CONFLICT OF INTEREST

The authors declare no conflict of interest.

DATA AVAILABILITY STATEMENT

All relevant data are included in the paper or its Supplementary Information.

REFERENCES

Anku, W. W., Mamo, M. A. & Govender, P. P. 2017 Phenolic compounds in water: sources, reactivity, toxicity and treatment methods. In: *Phenolic Compounds – Natural Sources, Importance and Applications* (Soto-Hernandez, M., Palma-Tenango, M. & del Rosario Garcia-Mateos, M., eds). IntechOpen, London. doi:10.5772/66927.

Arampatzidou, A. C. & Deliyanni, E. A. 2016 Comparison of activation media and pyrolysis temperature for activated carbons development by pyrolysis of potato peels for effective adsorption of endocrine disruptor bisphenol-A. *Journal of Colloid and Interface Science* **466**, 101–112.

Castro, C. S., Abreu, A. L., Silva, C. L. T. & Guerreiro, M. C. 2011 Phenol adsorption by activated carbon produced from spent coffee grounds. *Water Science & Technology* **64**, 2059–2065.

Cheng, W. P., Gao, W., Cui, X., Ma, J. H. & Li, R. F. 2016 Phenol adsorption equilibrium and kinetics on zeolite X/activated carbon composite. *Journal of the Taiwan Institute of Chemical Engineers* **62**, 192–198.

Crini, G. & Lichtfouse, E. 2019 Advantages and disadvantages of techniques used for wastewater treatment. *Environmental Chemistry Letters* **17**, 145–155.

Gao, X., Dai, Y., Zhang, Y. & Fu, F. 2017 Effective adsorption of phenolic compound from aqueous solutions on activated semi coke. *Journal of Physics and Chemistry of Solids* **102**, 142–150.

Giraldo, L. & Moreno-Piraján, J. C. 2014 Study of adsorption of phenol on activated carbons obtained from eggshells. *Journal of Analytical and Applied Pyrolysis* **106**, 41–47.

Hijab, M., Saleem, J., Parthasarathy, P., Mackey, H. R. & McKay, G. 2020 Two-stage optimisation for malachite green removal using activated date pits. *Biomass Conversion and Biorefinery* **11**, 727–740. doi:10.1007/s13399-020-00813-y.

Hui, T. S. & Zaini, M. A. A. 2015 Potassium hydroxide activation of activated carbon: a commentary. *Carbon Letters* **16**(4), 275–280.

Water Practice & Technology Vol 16 No 3
doi: 10.2166/wpt.2021.034

Khenniche, L. & Benissad-Aissani, F. 2010 Adsorptive removal of phenol by coffee residue activated carbon and commercial activated carbon: equilibrium, kinetics, and thermodynamics. *Journal of Chemical & Engineering Data* **55**, 4677–4686.

Laksaci, H., Khelifi, A., Belhamdi, B. & Trari, M. 2017 Valorization of coffee grounds into activated carbon using physic–chemical activation by KOH/CO_2. *Journal of Environmental Chemical Engineering* **5**, 5061–5066.

Lyman, D. J., Benck, R., Dell, S., Merle, S. & Murray-Wijelath, J. 2003 FTIR-ATR analysis of brewed coffee: effect of roasting conditions. *Journal of Agricultural and Food Chemistry* **51**, 3268–3272.

Ming-Twang, S., Lin-Zhi, L., Zaini, M. A. A., Zhi-Yong, Q. & Pei-Yee, A. Y. 2015 Activated carbon for dyes adsorption in aqueous solution. In: *Advances in Environmental Research*, Vol. 36 (Daniels, J. A., ed.). Nova Science Publishers, Inc., New York, NY, USA, pp. 217–234.

Mohammed, N. A. S., Abu-Zurayk, R. A., Hamadneh, I. & Al-Dujaili, A. H. 2018 Phenol adsorption on biochar prepared from the pine fruit shells: equilibrium, kinetic and thermodynamics studies. *Journal of Environmental Management* **226**, 377–385.

Rouquerol, J., Rouquerol, F., Llewellyn, P., Maurin, G. & Sing, K. S. W. 2013 *Adsorption by Powders and Porous Solids: Principles, Methodology and Applications*. Academic Press, London.

Shaid, M. S. H. M., Ahmad-Zaini, M. A. & Nasri, N. S. 2019 Evaluation of methylene blue dye and phenol removal onto modified CO_2-activated pyrolysis tyre powder. *Journal of Cleaner Production* **223**, 487–498.

Shu-Hui, T. & Zaini, M. A. A. 2016 Dyes – classification and effective removal techniques. In: *Advances in Chemistry Research*, Vol. 30 (Taylor, J. C., ed.). Nova Science Publishers, Inc., New York, NY, pp. 19–34.

Sing, K. S. W. 1982 Reporting physisorption data for gas/solid systems with special reference to the determination of surface area and porosity. *Pure and Applied Chemistry* **54**(11), 2201–2218.

Wang, J., Jun, S., Bittenbender, H. C., Gautz, L. & Li, Q. X. 2009 Fourier transform infrared spectroscopy for Kona coffee authentication. *Journal of Food Science* **74**, 385–391.

Wang, G., Zhang, S., Hua, Y., Su, X., Ma, S., Wang, J., Tao, Q., Wang, Y. & Komarneni, S. 2017 Phenol and/or Zn^{2+} adsorption by single- or dual-cation organomontmorillonites. *Applied Clay Science* **140**, 1–9.

Yan, K. Z., Ahmad-Zaini, M. A., Arsad, A. & Nasri, N. S. 2019 Rubber seed shell based activated carbon by physical activation for phenol removal. *Chemical Engineering Transactions* **72**, 151–156.

First received 29 October 2020; accepted in revised form 23 March 2021. Available online 31 March 2021